

Chapter 7

Modeling $I_2^-(OCS)_n$ Clusters

This chapter documents work in progress to develop a potential model for $I_2^-(OCS)_n$ clusters that can be used with the molecular dynamics simulation methods described in Chapter 2 to study the photodissociation of this system. The photofragmentation and photodissociation dynamics of $I_2^-(OCS)_n$ clusters have been investigated at 790 nm and 395 nm by Lineberger and coworkers [1, 2]. They have also conducted two-color pump-probe studies to gain more information about the cluster dynamics [3, 4].

7.1 Parametrizing the Interaction Hamiltonian

The model Hamiltonian discussed in Chapter 2 is a sum of the Hamiltonians of the isolated molecules, plus terms describing the solute–solvent and solvent–solvent interactions. Here we discuss the process of designing model potentials required for evaluating the interaction terms. These terms include long-range electrostatic and induction forces (Coulomb forces) and short-range dispersion and repulsion. In ionic systems we expect the long-range interactions to dominate the attractive region of the interaction potential. We therefore approximate the short-range interactions with state-independent pairwise potentials and rely on them primarily to set the repulsive wall of the potential in the correct place. As we will see below, the general approach for fitting our interaction potential is to calculate the long-range interactions using the model Hamiltonian and then seek out a short-range potential, which when added to the Coulombic in-

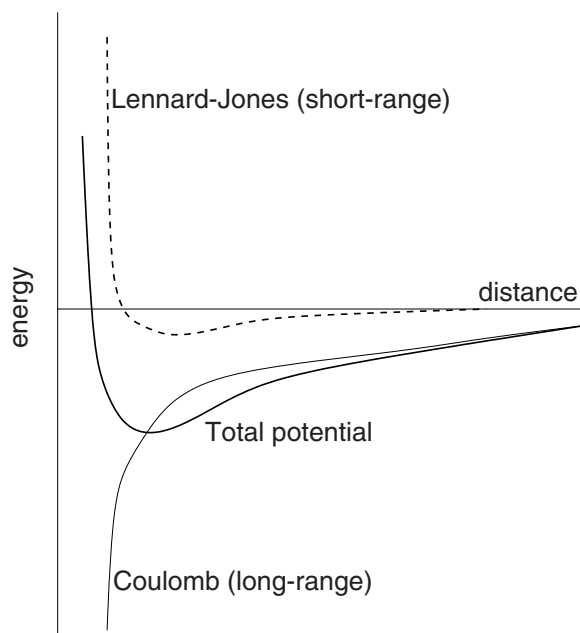


Figure 7.1: The solute–solvent, solvent–solvent interaction potential is a sum of the long-range Coulomb potential and short-range Lennard-Jones potential. The model parameters are chosen so that R_e and D_e of the total potential agree with known quantities.

interaction, produces a potential surface that has an equilibrium geometry (R_e and D_e) consistent with a known experimental or **ab initio** potential, see Fig. 7.1.

In our model, the solvent charge distribution is treated classically, represented by a distributed multipole expansion [5, 6]. For $I_2^-(CO_2)_n$ we have found that the five point charge model of Murthy et al. [7], combined with a single polarization site at the solvent center of mass provides an adequate description of the CO_2 charge distribution [6, 8]. We anticipate that a similar model will be acceptable for OCS. The short-range interactions in our model are typically treated by atom-atom Lennard-Jones potentials. The availability of empirical data to fit these potentials for OCS–OCS interactions is discussed in the following section.

To model the solute-solvent interactions, we also need to parametrize the short-range solute-solvent interactions. Since there is very little information available for interaction potentials of I_2^- with various solvents, we typically fit to data for interac-

tions of the solvent with the I^- and I fragments. Scattering data and photoelectron spectroscopy have been used to characterize these potentials for CO_2 and argon [9, 10], however this information is not available for OCS. This is the topic of the next section. Finally, we note that in modeling $I_2^-(CO_2)_n$, we find that the same short-range potentials can be used to describe the interaction of the solvent with both the I^- and neutral I fragments, and we assume this to be valid for OCS as well.

In summary, we need to select the following parameters for the solvent–solvent and solute-solvent interactions: point charges for OCS, molecular polarizability of OCS, Lennard-Jones parameters for O–O, C–C, S–S, O–C, O–S, C–S, I–O, I–C, and I–S.

7.2 Available Data

Ideally, we would fit our model potentials to experimentally determined values for equilibrium structures of $I(OCS)$, $I^-(OCS)$, $I_2^-(OCS)$ and $(OCS)_n$ clusters; however, very little empirical data is available for any of these systems. To the best of our knowledge, a recent **ab initio** calculation by Sanov et al. [1] represents all that is known about the I_2^-OCS and I^-OCS potentials. There are differing reports about the structure and binding energy of OCS dimer [11–13]. In this section, we describe the data available for the interactions we are modeling and in the following section we describe our attempts to reproduce what we believe are the most important attributes of these potentials.

Figure 7.2(b) shows a contour plot of the two-dimensional potential surface for $I^-(OCS)$ as determined from electronic structure calculations [1]. The global minimum of this potential surface corresponds to a linear configuration with sulfur nearest I^- . This dipole-bound minimum has a dissociation energy of 220 meV, and the S–I distance is 3.6 Å. There is a secondary, quadrupole-bound minimum, which is nearly T-shaped and bound by 67 meV. Calculations for $I_2^-(OCS)$ were performed at selected geometries

Table 7.1: Geometries and energies of OCS dimer minima

structure	R (Å)	Θ (deg)	Energy (meV)	
			MP2	model
Fig. 7.2(a)	3.6388	90.5	-60.9	-57.2
Fig. 7.2(b)	4.2529	47.1	-47.8	-44.8
Fig. 7.2(c)	3.9979	116.2	-48.8	-41.8
Fig. 7.3(a)	3.5665	88.5	–	-57.9
Fig. 7.3(b)	–	–	–	-65.6

and the minimum energy configuration was determined to be T-shaped with the sulfur end pointing toward the I_2^- waist. The dissociation energy for this complex is 137 meV, and the distance between sulfur and the I_2^- center of mass is 3.7 Å.

There is no consensus in the literature on the structure or binding energy of the OCS dimer. Molecular beam deflection studies by Lobue et al. [13] indicate that the dimer is polar, while IR absorption measurements by Randall et al. [12] conclude that the dimer is centrosymmetric. These conflicting results suggest the possibility that multiple, stable isomers of the dimer exist. **Ab initio** calculations by Bone suggest that the geometry reported by Randall et al. is the global minimum [11]; however, these calculations were restricted to planar geometries. Three configurations investigated in that study are shown in Fig. 7.3. All three structures correspond to stable points on the **ab initio** potential surface, and the configuration in Fig. 7.3(a) is most similar to the geometry reported by Randall et al. In two configurations the monomers are arranged antiparallel, one with the sulfur atoms internal, the other with the oxygen atoms internal. In the third configuration the monomers are parallel to one another. The energetics of these structures are given in Table 7.1. As discussed in the next section, we use these structures and energies as reference points for assessing the accuracy of the solvent-solvent interactions in our model potential.

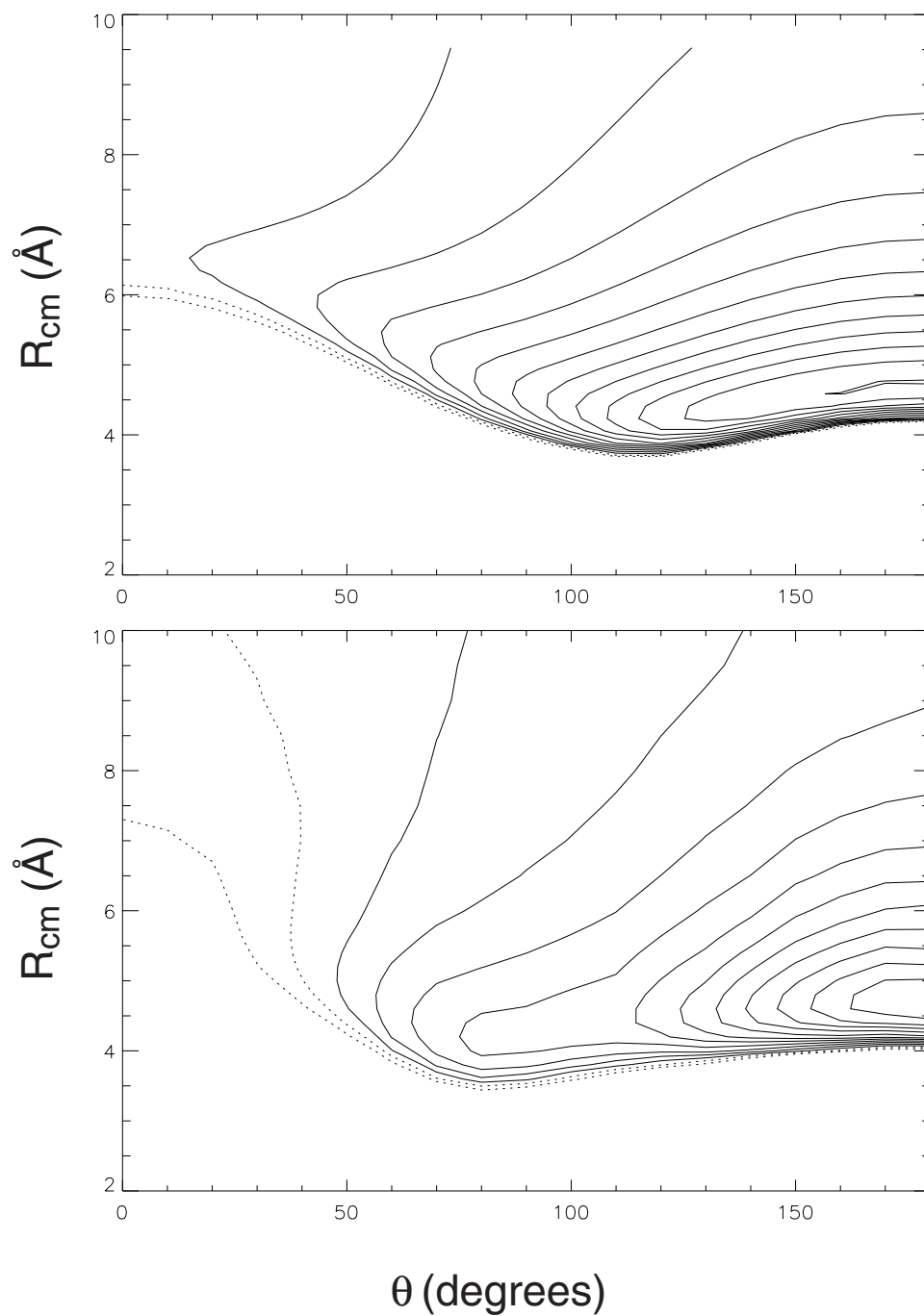


Figure 7.2: Two-dimensional contour plots of the I^- (OCS) potential from (a) our interaction model, and (b) the electronic structure calculation of Ref. 1.

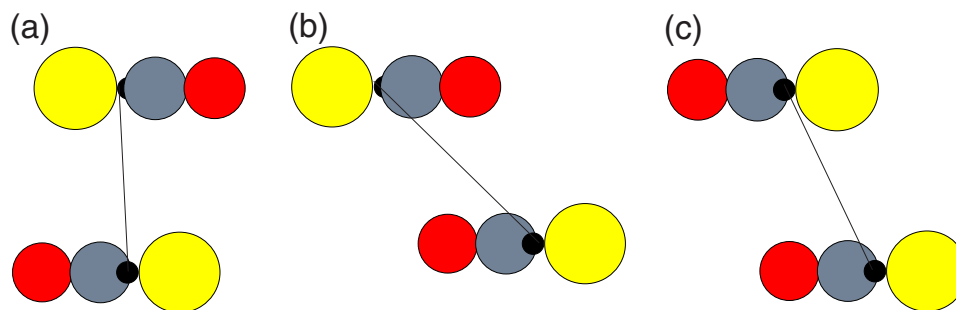


Figure 7.3: Stable structures for the OCS dimer calculated by Bone.

Table 7.2: Model parameters for OCS

atom	charge (a.u.)	Lennard-Jones parameters for interaction with I σ (a.u.)	ϵ (a.u.)
O	-0.07663	8.5	6×10^{-4}
C	+0.03816	8.5	6×10^{-4}
S	+0.03847	7.1	6×10^{-4}

7.3 Fitting Parameters

We assign a three point charge model for OCS by solving a system of linear equations for the charge, dipole and quadrupole moments of OCS, which are 0, 0.7152 D and -0.79 D \AA , respectively [14]. The resulting charges on each nucleus are listed in Table 7.2. We note that this is an overly simple method for selecting point charges and we do not expect it to describe the OCS charge distribution accurately; however, it serves as a starting point. The molecular polarizability, $\alpha = 5.21 \text{ \AA}^3$ and the polarizability anisotropy, $\gamma = 4.67 \text{ \AA}^3$ [14], were used to determine the parallel and perpendicular polarizabilities of 58.5 au and 25.7 au, respectively.

With this model for OCS, we calculate the electrostatic and induction energy of linear I^- —SCO as a function of the I—S distance. In this case, the charge distribution of I^- is also classical and is modeled by a single charge of $-e$ at the iodine nucleus. The Coulombic interaction energy for this system is shown in Fig. 7.4.

The basic method of handling the short-range interactions places isotropic, pair-

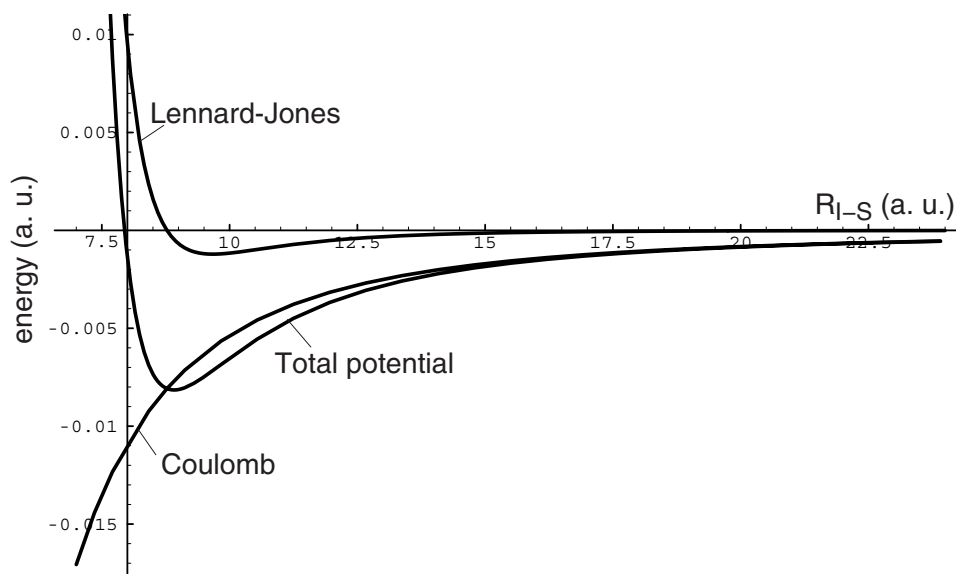


Figure 7.4: Sum of long-range and short-range contributions to model interaction potential, with parameters fit to reproduce the calculated equilibrium I^- —S distance of 3.6 Å and well depth of 220 meV.

wise Lennard-Jones (LJ) sites on all the nuclei,

$$\hat{H}^{\text{sr}} = \sum'_{ij} 4\epsilon_{ij} \left(\frac{\sigma_{ij}^{12}}{R_{ij}^{12}} - \frac{\sigma_{ij}^6}{R_{ij}^6} \right), \quad (7.1)$$

where the indices i and j run over all the atomic sites in the system, and the sum is restricted to include only pairs where the sites reside on different molecules. Since the global minimum of the I^- (OCS) potential corresponds to a linear configuration with sulfur nearest I^- , we expect σ_{IS} and ϵ_{IS} to be the most important parameters in determining the short-range interaction potential. Initially, we used the I–O and I–C parameters fit for $\text{I}_2^-(\text{CO}_2)_n$ clusters and varied the I–S parameters to reproduce the equilibrium geometry determined by the electronic structure calculation. The well depth and equilibrium bondlength of the total potential in Fig. 7.4 are 220 meV and 3.6 Å, as desired.

Next, we sought to reproduce secondary features of the calculated potential using the same general technique, but mapping the surface in two dimensions: \mathbf{R} is the distance from I^- to the OCS center of mass, and θ is the angle between \mathbf{R} and the

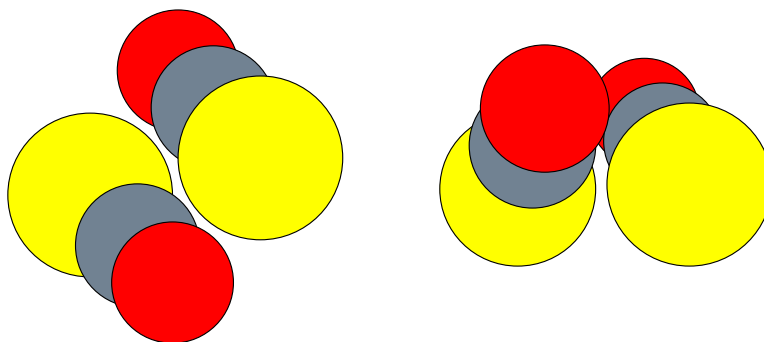


Figure 7.5: Structures for the OCS dimer calculated from the model interaction potential. (a) Planar, bound by 60 meV. (b) Nonplanar, bound by 65 meV.

O–C bond. The I–O and I–C parameters given in Table 7.2 were selected to create a repulsive potential as I^- approaches the O end of OCS and to match the energy of the t-shaped configuration found in the **ab initio** calculation. However, the shape of the model potential, seen in Fig. 7.2, clearly differs from the *ab initio* potential. In particular, bending about the I^- –SCO minimum is too facile in the model potential. Consequently, the $I_2^-(\text{OCS})$ binding energy is about 230 meV, considerably larger than determined from the electronic structure calculation [1]. Experimentation with a wide range of Lennard-Jones parameters indicated that the angular dependence of the $I^-(\text{OCS})$ potential cannot be significantly improved in this manner. Alternatively, we propose improving the crude electrostatic model for OCS, as discussed below.

Lennard-Jones parameters for OCS–OCS interactions were taken from simulations of liquid OCS [15, 16]. Table 7.1 compares the energy of the OCS dimer calculated by our model potential to the MP2/TZ2P BSSE-corrected results of Bone’s **ab initio** calculation at three of the geometries considered in that work [11]. While the agreement is not too bad, none of these geometries correspond to minima on our potential surface. We find two low-lying minima, shown in Fig. 7.5. The structure on the left is bound by about 60 meV, comparable to the minimum calculated by Bone, but the second structure is X-shaped (nonplanar) and bound by 65 meV. At this point it is

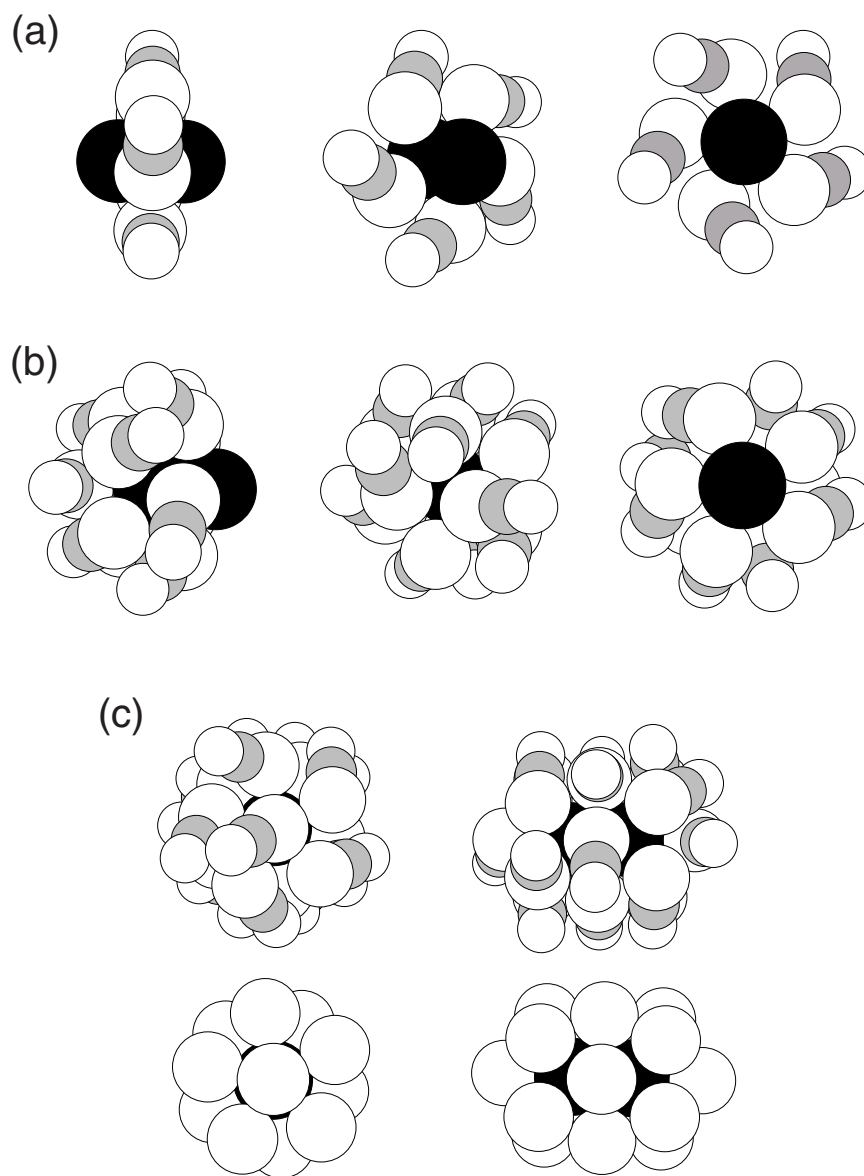


Figure 7.6: Calculated structures for $I_2^-(OCS)_n$ clusters. (a) $n = 5$. (b) $n = 11$. (c) $n = 17$, also shown with C and O removed.

unclear whether this is an artifact of our potential model or if this isomer exists.

7.4 Results for $I_2^-(OCS)_n$

Using the above model to determine structures for $I_2^-(OCS)_n$, we find that OCS molecules arrange themselves first about the waist of I_2^- with the sulfur ends nearest

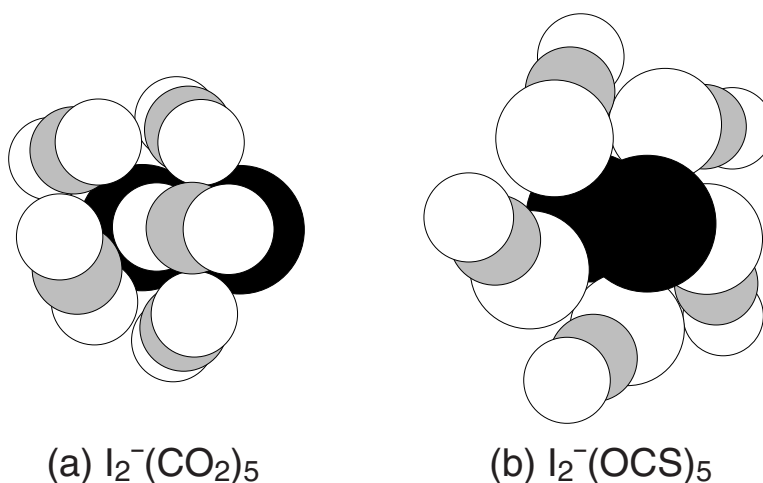


Figure 7.7: Comparison of cluster structures for $I_2^-(CO_2)_5$ and $I_2^-(OCS)_5$.

the solute. The solvent molecules are tilted towards one another, rather than pointing radially outward, see Fig. 7.6(a). The sulfur atoms are 3.57 Å from the I_2^- center of mass. Five OCS molecules complete a ring around I_2^- . Additional OCS molecules form a second ring around one end of the solute, then a single OCS molecule fills the axial site, completing the half-shell structure shown in Fig. 7.6(b). The other side is filled in the same fashion, completing the first solvent shell at $n = 17$, shown in Fig. 7.6(c). The $n = 17$ structures are also shown with carbon and oxygen removed to reveal the underlying structure.

In contrast, for $I_2^-(CO_2)_n$ clusters, discussed in Chapter 3, the dominant charge-quadrupole interactions result in CO_2 molecules lying flat with respect to I_2^- . In small clusters, CO_2 molecules pack together on one side of the I_2^- core rather than forming a ring. A comparison of the $n = 5$ cluster for the two solvents is shown in Fig. 7.7.

In the current model, the $I_2^-(OCS)$ interaction energy is overestimated. As the model improves, and this energy is reduced, we expect the OCS–OCS interaction to become more important in determining the packing of solvent molecules around I_2^- . For the model described here, secondary minima for the $I_2^-(OCS)_5$ cluster feature solvent molecules clustered on one side of I_2^- rather than forming a ring structure. The energy

of this configuration is -1.17 eV, compared to -1.21 eV for the ring structure. However, OCS is fundamentally different from CO₂ in that OCS points carbon and oxygen away from I₂⁻ while CO₂ lies on its side with carbon nearest the solute. Overall, we expect that the underlying structure of sulfur atoms in $n = 17$ will persist as the model is improved, but the tilt of OCS could change significantly, and we would not be surprised to see smaller clusters with OCS molecules localized on one side of I₂⁻.

We have performed limited studies of the dynamics with this model. Photodissociation simulations of I₂⁻-(OCS)₆ at 790 nm were computed for an ensemble of 100 trajectories. We observed 70% caging, compared to 40% caging in the experiment [1]. This tells us that the interaction model is inadequate, but doesn't tell us what needs to be improved. However, we expect that the three point charge model for the OCS charge distribution is the weakest aspect of the current model.

7.5 Recommendations for Improving the Model

We have not found a five point charge model for OCS in the literature, however, Randall et al. report a five point distributed multipole expansion for the OCS charge distribution which includes charge, dipole and quadrupole moments [12]. The current implementation of our model is not coded to compute the long-range interaction terms of order R^{-5} , which would be required to include the quadrupole-quadrupole contributions to the interaction. This would be a straightforward modification, but the disadvantage would be a considerable increase in the computing time required. This could prove to be prohibitive for running dynamics simulations of moderate-sized clusters. Perhaps a better approach would be to develop a five point charge model, derived from the larger multipole expansion.

As a preliminary test, we used the electrostatic model of Randall et al. to calculate the long-range I⁻-(SCO) interaction, excluding terms of order R^{-4} and higher and fit I-OCS Lennard-Jones parameters for this model. We were able to greatly improve

the shape of our potential, particularly with regard to stiffening the I^- —SCO bend. The I_2^- (OCS) binding energy was lowered to 160 meV, much closer to the **ab initio** value of 137 meV. Unfortunately, this model gave unreasonable results for the solvent-solvent interactions. We were unable to reproduce any of the reported structures for the OCS dimer, despite attempts to calculate the structures using another program, Orient [17], which is designed to include terms of the order, R^{-5} . The source of error has not been determined, but the general lesson is that an improved model for the OCS charge distribution appears to be the best way to improve the overall interaction potential.

References for Chapter 7

- [1] S. Nandi, A. Sanov, N. Delaney, J. Faeder, R. Parson, and W. C. Lineberger, *J. Phys. Chem. A* **102**, 8827 (1998).
- [2] A. Sanov, T. Sanford, S. Nandi, and W. C. Lineberger, *J. Chem. Phys.* **111**, 663 (1999).
- [3] A. Sanov and W. C. Lineberger, private communication.
- [4] A. Sanov, S. Nandi, and W. C. Lineberger, *J. Chem. Phys.* **108**, 5155 (1998).
- [5] A. J. Stone, *The Theory of Intermolecular Forces*, Oxford, New York, 1996.
- [6] J. Faeder, N. Delaney, P. Maslen, and R. Parson, *Chem. Phys.* **239**, 525 (1998).
- [7] C. S. Murthy, K. Singer, and I. R. McDonald, *Mol. Phys.* **44**, 135 (1981).
- [8] N. Delaney, J. Faeder, P. E. Maslen, and R. Parson, *J. Phys. Chem. A* **101**, 8147 (1997).
- [9] Y. Zhao, C. C. Arnold, and D. M. Neumark, *J. Chem. Soc. Faraday Trans.* **89**, 1449 (1993).
- [10] Y. Zhao, I. Yourshaw, G. Reiser, C. C. Arnold, and D. M. Neumark, *J. Chem. Phys.* **101**, 6538 (1994).
- [11] R. G. A. Bone, *Chem. Phys. Lett.* **206**, 260 (1993).
- [12] R. W. Randall, J. M. Willkie, B. J. Howard, and J. S. Muentner, *Mol. Phys.* **69**, 839 (1990).
- [13] J. M. Lobue, J. K. Rice, and S. E. Novick, *Chem. Phys. Lett.* **112**, 376 (1984).
- [14] C. G. Gray and K. E. Gubbins, *Theory of Molecular Fluids*, volume 1, Clarendon, Oxford, 1984.
- [15] H. Stassen, T. Dorfmueller, and J. Samios, *Mol. Phys.* **77**, 339 (1992).
- [16] J. Samios and H. Stassen, *Chem. Phys.* **170**, 193 (1993).
- [17] ORIENT, a program for studying interactions between molecules by A. J. Stone, A. Dullweber, P. L. A. Popelier, and D. J. Wales, version 3.2 (1995).